ISBN: 978-3-95450-232-5 ISSN: 2673-7000 doi:10.18429/JACoW-NAPAC2022-WEPA04

SIMULATING TWO DIMENSIONAL TRANSIENT COHERENT SYNCHROTRON RADIATION IN JULIA

W. Lou*, C. Mayes, Y. Cai, SLAC National Accelerator Laboratory, Menlo Park, CA, USA

Abstract

Coherent Synchrotron Radiation (CSR) in bending magnets poses a potential limit for electron beams to reach high brightness in novel accelerators. While the longitudinal wakefield has been well studied in one-dimensional CSR theory and implemented in various simulation codes, transverse wakefields have received less attention. Following the recently developed two and three-dimensional CSR theory, we developed software packages in Python and Julia to simulate the 2D CSR effects. The Python packages, PyCSR2D and PyCSR3D, utilize parallel processing in CPU to compute the steady-state CSR wakes. The Julia package, JuliaCSR2D, additionally computes the 2D transient CSR wakes with GPU compatibility. We applied these codes to simulate the 2D CSR effects in the FACET-II particle accelerator at the SLAC National Accelerator Laboratory.

INTRODUCTION

When an electron traverses a curved trajectory, synchrotron radiation is emitted and can apply energy kicks to the other electrons in the same bunch. The low frequency components of the radiation spectrum, with wavelengths on the order of the bunch length, can add coherently, and is termed coherent synchrotron radiation (CSR). CSR can result in undesired effects including increase in energy spread and beam emittance, energy loss, and potential microbunching instability. For a beam with high bunch charge Q and short bunch length σ_z, the effects tend to be more severe. Because the current FACET-II chicane design at SLAC calls for great longitudinal beam compression ($Q \sim 2$ nC, $\sigma_z \sim 0.5\,\mu$m at the final bunch compressor, CSR effects can be significant [1].

For fast computation, many simulation codes apply only the one-dimensional CSR model while neglecting the 2D/3D CSR effects. The negligence is considered acceptable if the transverse beamsizes $\sigma_{x,y}$ satisfy $\sigma_{x,y} \ll \sigma_z^{2/3}\rho^{1/3}$, where ρ is the bending radius [2]. However in the middle of the FACET-II BC2 chicane compressor, this limit is not satisfied, and inclusion of the 2D/3D effects might be necessary. The 2D/3D CSR theory with a constant ρ has been recently developed in [3, 4]. In 2021 we developed Python codes, *PyCSR2D* and *PyCSR3D*, to efficiently compute the steady-state (s-s) wakes [5–7]. This paper shows how we developed codes in Julia to efficiently calculate the 2D *transient* wakes based on the theory, including the entrance and exit wakes within a bending magnet. The code is named *JuliaCSR2D*, and is open-source on Github [8]. The benchmarking results with 1D transient CSR theory and tracking results with the FACET-II chicane are also presented here.

* wlou@slac.stanford.edu

2D TRANSIENT WAKE COMPUTATION

The 2D transient longitudinal and horizontal CSR wakes solved in [3] are given in the form of:

$$W_s(z,x) = \int_{-\infty}^{\infty} dx' \int_{z-g(x-x')}^{z-f(x-x')} dz' E_s(\tfrac{z-z'}{2\rho}, \tfrac{x-x'}{\rho})\,\lambda_b(z',x'),$$

$$W_x(z,x) = \int_{-\infty}^{\infty} dx' \int_{z-g(x-x')}^{z-f(x-x')} dz' E_x(\tfrac{z-z'}{2\rho}, \tfrac{x-x'}{\rho})\,\lambda_b(z',x'),$$

in which λ_b is the bunch distribution, and E_s and E_x are the longitudinal and horizontal *fields* solved in terms of ρ and the relativistic γ. The fields and the functions in the integration limits (f and g) take different forms depending on the location of the observation point (z,x) and the source point (z',x'). When the observation point is located inside the bending magnet, the wakes are called the *entrance* wakes. For a Gaussian bunch, the longitudinal entrance wake becomes the s-s wake when the observation point traverses beyond the over-taking distance $L_0 = (24\sigma_z\rho^2)^{1/3}$. Thus for a short magnet, the s-s might not be reached. When the observation point is located downstream to the magnet, the wakes are called the *exit* wakes.

In the s-s case, these integrals can be efficiently computed numerically by using an FFT-based convolution [7]. However this trick is no longer valid due to the *finite* limits in the dz' integral. Moreover, the field functions (E_s and E_x) have severe numerical spikes or singularities around $z' \sim z$, especially for large γ. To numerically resolve the spikes, we apply the Tanh-Sinh Quadrature (QTS) method to evaluate the dz' integrals [9]. QTS allows the integrand to decay at the two boundaries with a double exponential rate. To ensure consistent convergence with various parameters, effort was spent in developing an algorithm to numerically

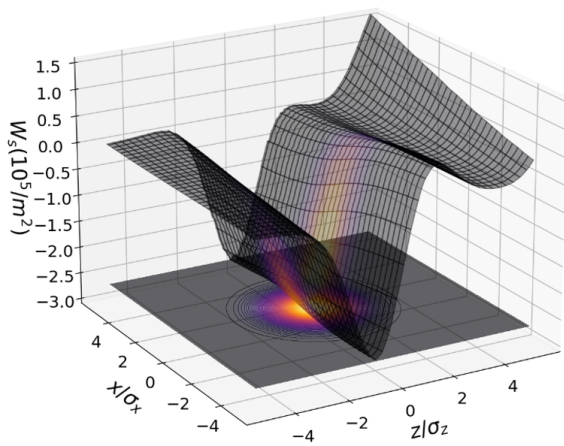

Figure 1: A contour plot of the longitudinal entrance wake $W_s(z,x)$ of a Gaussian bunch distribution. Parameters used: $\gamma = 10,000$, $\rho = 1.5$ m, $\sigma_z = \sigma_x = 0.5\,\mu$m.

ISBN: 978-3-95450-232-5 ISSN: 2673-7000 doi:10.18429/JACoW-NAPAC2022-WEPA04

find the spike locations and place them on the integration boundaries. We call these locations the *break points*. Once the dz' integral converges, we simply perform a discrete 1D summation for the dx' integral. Figure 1 and Figure 2 show respectively the computed W_s and W_x entrance wake grids at an entrance angle of $\phi = 0.11$ rad using a Gaussian bunch of 5 million particles ($N_p = 5 \times 10^6$).

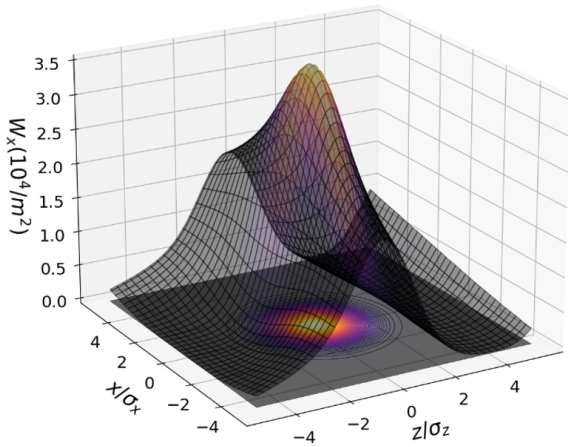

Figure 2: A contour plot of the horizontal entrance wake $W_x(z, x)$ of a Gaussian bunch distribution. Parameters used are the same as in Fig. 1.

CONVERGENCE TEST

In JuliaCSR2D there are two numerical parameters controlling the integration resolution: the longitudinal resolution is controlled by M, while the horizontal resolution is controlled by n_{xp}. For each x', we perform either one or two 1D QTS integrals in the z' direction. The number of integration points for each QTS integral is approximately 3.125×2^M. The number of integrals to sum in the x' direction is n_{xp}. Both M and n_{xp} are integers.

Figure 3 shows the computed longitudinal entrance wake at the bunch center $W_s(z = 0, x = 0)$ with various M and n_{xp}, for $\phi = 0.01$ rad and 0.05 rad respectively. Because the true value of W_s is unknown, we use the computed value with the highest integration resolution ($M = 10, n_{xp} = 1000$) as the reference value. In general, the computed wake values converge as M and n_{xp} increase. For a small entrance angle (typically $\phi < 0.02$ rad), the convergence requires larger M and n_{xp} values. For a large entrance angle ($\phi > 0.03$ rad),

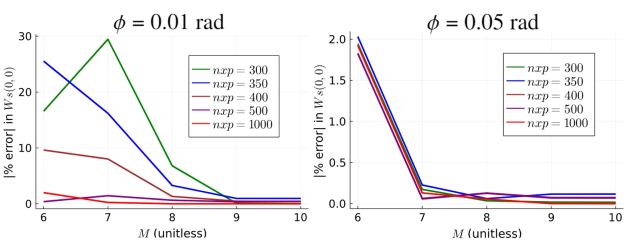

Figure 3: Convergence test for $Ws(0, 0)$ at an entrance angle of $\phi = 0.01$ rad (left) and $\phi = 0.05$ rad (right). Parameters used are the same as in Fig. 1.

using $M = 7$ and $n_{xp} = 300$ is usually enough to achieve a relative error below 1%. The convergence behavior of the *exit* wakes depends similarly on the total bending angle of the magnet ϕ_m. Large M and n_{xp} values are required if ϕ_m is too small. Note that the convergence behavior depends on γ and ρ too, so a convergence test is highly recommended when lattice parameters vary. Note that the computation time is approximately proportional to $n_{xp} \times 2^M$.

BENCHMARKING WITH 1D CSR THEORY

In this section we benchmarked the computed transient wakes using JuliaCSR2D within one bending magnet with the 1D CSR theory. For consistency we used the same Gaussian beam ($N_p = 5 \times 10^6$) and lattice parameters as in Fig. 1. Figure 4 shows the agreement between the computed longitudinal entrance wake $W_s(z, x = 0)$ and the prediction from the 1D theory. As the entrance angle ϕ increases from 0 to about 0.8 rad, the wake amplitude continues to grow. As ϕ further increases, the top peak begins to drop in amplitude and "leaves" the visible range of the bunch. The top peak of the wake still exists outside $z > 5\sigma_z$, but no longer contributes to kick the bunch. Such propagation behavior has been observed in [10]. At $\phi = 0.2$, the wake has reached the steady state.

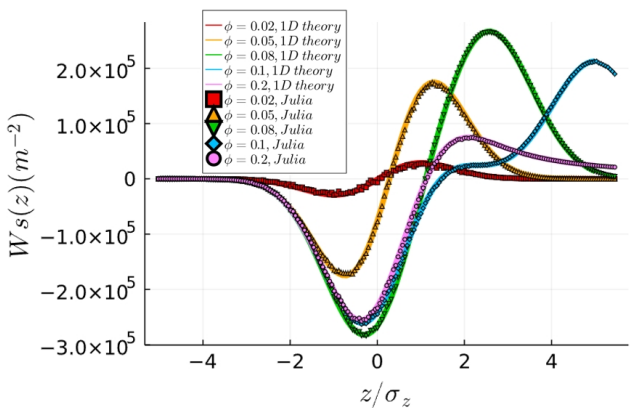

Figure 4: Benchmarking the longitudinal entrance wake propagation computed from JuliaCSR2D $W_s(z, 0)$ with the 1D CSR theory.

Similar to Fig. 4, Figure 5 shows the agreement for the exit wake. As the exit distance $\lambda\rho$ increases, the wake amplitude drops as expected. Note that for JuliaCSR2D, the exit wake includes the contribution where the source particles are between the magnet's exit and the observation point. This contribution is neglected in the 1D theory, but is required for the 2D exit wake computation to agree with the 1D theory. Details regarding this extra contribution are shown in [3].

SLAC FACET-II CHICANE TRACKING

To find out the effects from transient CSR wakes, we applied JuliaCSR2D on the FACET-II chicane design lattice. Note that a similar study has been performed with PyCSR2D in [7]. The lattice and beam parameters are: $E = 30$ GeV, $\rho = 1538$ m, $L_{\text{bend}} = 20$ m, and $L_{\text{drift}} = 32.5$ m, $Q = 2$ nC,

ISBN: 978-3-95450-232-5 ISSN: 2673-7000 doi:10.18429/JACoW-NAPAC2022-WEPA04

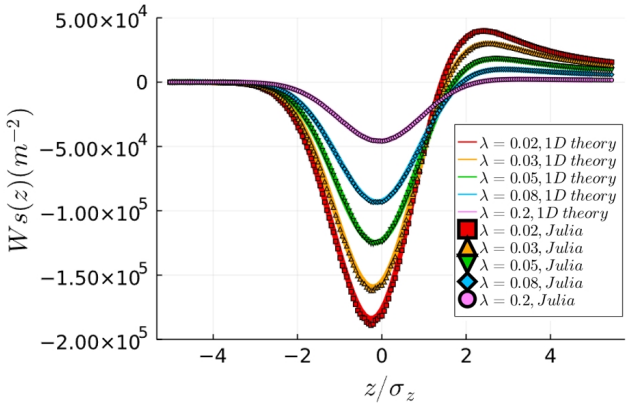

Figure 5: Benchmarking the longitudinal exit wake propagation computed from JuliaCSR2D $W_s(z, 0)$ with the 1D CSR theory. λ is the exit distance divided by ρ.

$\sigma_z = 40\,\mu m$, $\sigma_x = 134\,\mu m$. The initial beam is a Gaussian with energy chirp and $N_p = 10^6$ macro-particles. Figure 6 shows the projected horizontal emittances on a logarithmic scale as the bunch traverses the chicane with different CSR settings. As expected, the final bending magnet contributes the most emittance growth because the CSR effects scale up with a compressed σ_z. While the horizontal CSR wake is weaker than the longitudinal wake, it still noticeably contributes to the increase in beam emittance. The contribution from the exit wake is also significant and should not be neglected. Figure 7 shows the longitudinal and horizontal phase space plots at the end of chicane tracking, with either "energy kick only" or "both kicks on". The additional transient horizontal CSR wake results in significant differences.

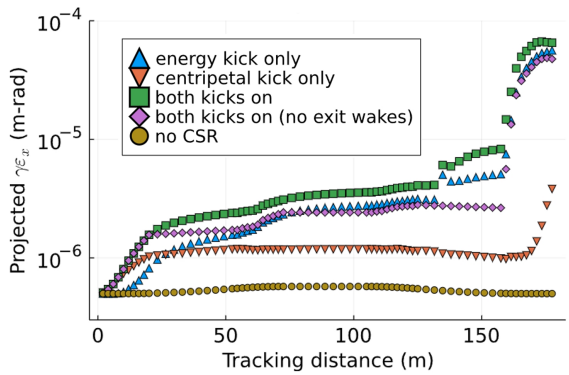

Figure 6: Projected horizontal beam emittance of a Gaussian bunch traversing the FACET-II chicane with 2D transient CSR wakes applied from JuliaCSR2D. Each curve corresponds to a different CSR setting.

CODE SPEED-UP, APPLICABILITY AND FUTURE STEPS

The main reason we switched code development from Python to Julia is the convenient GPU applicability on Julia. To achieve this, all the elementary codes have been made GPU-compatible, including QTS integration and 2D

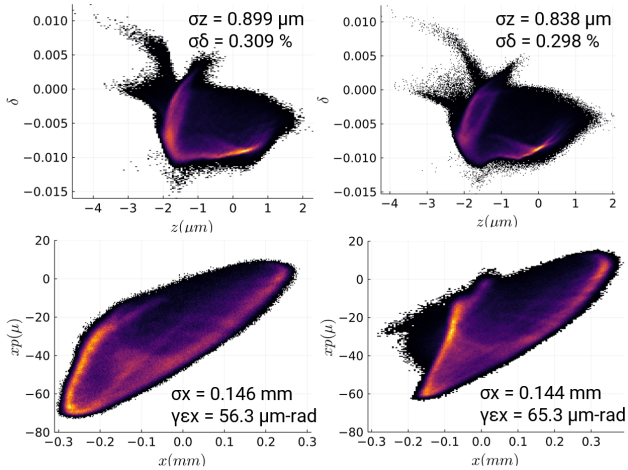

Figure 7: Longitudinal (top) and horizontal phase space (bottom) plots at the end of FACET-II chicane tracking with either energy kick only (left) or both kicks on (right). The tracking result with 1D CSR is similar to that with the energy kick only (not shown here).

interpolation. Transient wake computation on JuliaCSR2D using *NVIDIA A100* GPU is approximately 100x faster than the equivalent calculation on a multi-core (64) CPU. With $M = 7$ and $n_{xp} = 300$, the wake computation per tracking step takes the GPU less than 40 seconds. Currently the computed wakes could be inaccurate if the entrance angle is too small ($\phi < 0.02$). This can usually be fixed by including more macro-particles in the bunch ($N_p > 5 \times 10^6$), or increasing the integration resolution ($M > 7$ and $n_{xp} > 500$). However both methods increase the computation time. Future steps for JuliaCSR2D include adding the space-charge wake calculation, and applying multiple GPUs for further speed-up.

CONCLUSION

We have developed Julia codes called JuliaCSR2D to efficiently compute the 2D transient CSR wakes. The codes are made GPU compatible to speed up the computation. The codes have been benchmarked with the 1D CSR theory, and tracking results for the FACET-II chicane show that both entrance and exit wakes contribute to the emittance growth, and transverse wakes can have significant effects on the beam.

ACKNOWLEDGEMENTS

This work has been supported by the U.S. Department of Energy Office of Science, Office of Basic Energy Sciences under Contract No. DE-AC02-76SF00515. This research used resources of the National Energy Research Scientific Computing Center (NERSC), a U.S. Department of Energy Office of Science User Facility located at Lawrence Berkeley National Laboratory, operated under Contract No. DE-AC02-05CH11231 using NERSC award BES-ERCAP0016827 for 2021.

ISBN: 978-3-95450-232-5 ISSN: 2673-7000 doi:10.18429/JACoW-NAPAC2022-WEPA04

REFERENCES

[1] V. Yakimenko *et al.*, "FACET-II facility for advanced accelerator experimental tests", *Phys. Rev. ST Accel. Beams*, vol. 22, p. 101301, 2019. doi:10.1103/PhysRevAccelBeams.22.101301

[2] S. Derbenev *et al.*, "Microbunch radiative tail-head interaction", TESLA, Tech. Rep. TESLA-FEL-95-05, 1995.

[3] Y. Cai and Y. Ding, "Three-dimensional effects of coherent synchrotron radiation by electrons in a bunch compressor", *Phys. Rev. ST Accel. Beams*, vol. 23, p. 014402, 2020. doi:10.1103/PhysRevAccelBeams.23.014402

[4] Y. Cai, "Two-dimensional theory of coherent synchrotron radiation with transient effects", *Phys. Rev. ST Accel. Beams*, vol. 24, p. 064402, 2021.

[5] PyCSR2D, https://github.com/weiyuanlou/PyCSR2D/

[6] PyCSR3D, https://github.com/ChristopherMayes/PyCSR3D/

[7] W. Lou, C. Mayes, Y. Cai, G. White, "Simulating two dimensional choherent synchrotron radiation in Python", https://epaper.kek.jp/ipac2021/papers/wepab234.pdf/

[8] JuliaCSR2D, https://github.com/weiyuanlou/JuliaCSR2D/

[9] Tanh-sinh quadrature, https://en.wikipedia.org/wiki/Tanh-sinh_quadrature/

[10] G. Stupakov and P. Emma, "CSR wake for a short magnet in ultrarelativistic limit", SLAC-PUB-9242, https://www.slac.stanford.edu/pubs/slacpubs/9000/slac-pub-9242.pdf